



Influence of bone marrow-derived mesenchymal stem cells versus low-level laser irradiation therapy on the rat parotid glands after streptozotocin-induced diabetes .

Ashraf Mohamad Emran*, Said Mahmud Hani**, and Sayed Bakry Ahmed** *

* Assistant lecturer of oral histology, Oral Biology Department, Faculty of Dental Medicine, Al-Azhar University

** Professor of Oral Histology and Pathology, Oral Biology Department, Faculty of Dental Medicine, Al-zhar University.

** Professor, Department of Zoology, Dean of Faculty of Science, Al-Azhar University.

Abstract:

Objective: The current study was designed to assess the therapeutic effect of bone marrow-derived mesenchymal stem cells (BMSCs) versus low-level laser therapy (LLLT) on the rat parotid glands after streptozotocin induced diabetes in rats. **Materials and Methods:** 48 Sprague-Dawley rats were divided into 4 groups, 12 rats each. **Group I:** the animals received 0.1 M sodium citrate buffer intraperitoneally, the vehicle of streptozotocin. **Group II:** diabetes mellitus was induced by single intraperitoneal injection of 60 mg/kg of streptozotocin (STZ) dissolved in 0.1 M sodium citrate buffer. **Group III:** one day after diabetes induction, single dose of 2×10^6 BMSCs suspended in 0.5 ml of phosphate buffer solution (PBS) was injected via intraglandular route. **Group IV:** one day after diabetes induction; the animals were exposed to single session of LLLT on the right parotid gland area. Animals were sacrificed at 7 or 14 days after BMSCs injection or laser irradiation parotid glands were harvested, then histological and immunohistochemical studies were performed. **Result:** The experimental stem cell treated group showed better histological features and more PCNA proliferation than the laser treated group. **Conclusion:** bone marrow derived stem cell and laser treatment are successful method in the treatment of diabetic induced salivary gland injury, with relative superiority of stem cell treatment.

Key words: parotid gland, stem cells, laser- therapy, diabetes.

I. Introduction

Diabetes mellitus (DM) is a general term for heterogeneous disturbances of carbohydrate metabolism contribute to the main findings of chronic hyperglycemia. The cause of diabetes is either impaired insulin secretion or impaired insulin action or both ⁽¹⁾. The DM is actually not a disease but rather a syndrome made up of several manifestations which have similar symptoms, signs, and complications, particularly hyperglycemia, but with different etiologies. The chronic hyperglycemia of diabetes is associated with long-term damage, dysfunction, and failure in the function of different organs, especially the eyes, kidneys, nerves, heart, and blood vessels ⁽²⁾.

Diabetes and insulin change both the structure and function of rat parotid glands. The parotid glands of diabetic animals are morphologically characterized by extensive intracellular lipid accumulation in the acinar cells with increased lysosomes, duplication and thickening of the basement membranes and crystalloids inclusions^(3,4).

The STZ is a fungal antibiotic, with ability to induce insulin- and non-insulin- dependent DM via β -cell destruction. A single dose of either intravenous or intraperitoneal injection of 40-60 mg/kg of STZ is reported to be sufficient to induce insulin dependent DM in adult rats⁽⁵⁾.

A previous study has revealed that the BMSCs can increase the regenerative capacity of the resident salivary gland stem cells that have remained in the damaged salivary glands upon the degenerative state⁽⁶⁾. So that it seemed that BMSCs could exert direct proliferative effect on salivary gland cells as well as the indirect effect via stimulating the survived stem cells resident in the gland. The stem cell therapy for the repair and functional restoration of salivary glands could provide long-term and effective solution to the damaged tissues induced by the degenerative processes either due to the age-related changes or the disease⁽⁷⁾. The BMSCs showed the ability to differentiate into epithelial cells *in vitro* and they also showed the regenerative power to restore both the lost normal morphology as well as the function by secreting bioactive factors. These factors are believed to create a repair environment through their antiapoptotic effects, immunoregulatory function and stimulation of endothelial progenitor cell proliferation that helps in vascularization of the damaged tissue^(8,9).

The Low- level laser (LLL) has been widely used for wound healing, pain reduction and the treatment of inflammation⁽¹⁰⁾. Significant salivation improvement, both quantitatively and qualitatively, was obtained upon the treatment of the major salivary glands of xerostomia patients with LLL on 10 occasions⁽¹¹⁾. Other investigation has revealed that the effects of LLL on salivary glands were not only stimulating, but also, relatively regenerative since the glandular response to the same amount of applied laser energy increased linearly over time⁽¹²⁾.

II. Materials and Methods

2.1. Animals and experimental design: The protocol of this study was approved by the Bioethics Committee of Animals, from the Faculty of Dentistry, Al-Azhar university. The animal handling and the procedures application were carried out at the House Animals of Cairo University. The animals were caged individually with free access to water and food.

The present study was carried out on adult male SpragueDawley rats with average age around 2 months old and weighted 200 to 250 gm. The selection of male gender since there is a strong affection of the laboratory animal gender on the ability of STZ to induce DM, where the male laboratory animals, including rats, were more prone to the effect of STZ to induce DM than females⁽¹³⁾. The present study has utilized male animals in order to avoid the aforementioned obstacle as well as the effects of female sex hormones changes.

2.2. Animal grouping: After 48 hours fasting overnight, the animals received STZ injection, 48 rats were divided into 4 groups, 12 rats each, in the following scheme:

- **Group I (GI):** control group; was considered as the negative control; in which the animals received 0.1 M sodium citrate buffer (SCB) intraperitoneally that is the vehicle of streptozotocin.
- **Group II (GII):** diabetic group, was considered as the positive control in which the diabetes mellitus was induced by a single intraperitoneal injection of 60 mg/kg of streptozotocin (STZ) (Sigma Chemical Co., St. Louis, MO) dissolved in 0.1 M (SCB)⁽¹⁴⁾. The blood samples were examined daily until diabetes was established. when after 12 hours fasting, the rats have reached a serum postprandial glucose level of >250 mg/dl⁽¹⁵⁾. So, the rats were considered as diabetic and were included into both the diabetic and the subsequent therapeutic groups.
- **Group III (GIII):** stem cells group, one day after diabetic induction, as described in group II, BMSCs with

a dose of 2×10^6 cells⁽¹⁶⁾ suspended in 0.5 ml of phosphate buffer solution (PBS) was injected via intraglandular route in a single injection into the right parotid gland region.

- **Group IV (G IV):** laser group; one day after diabetes induction, the animals were exposed to single session of LLLT on the right parotid gland area.

Each group was divided into two sub-groups A and B according to the time of scarification, A: at 7-day, and B at 14 -days after diabetes induction which was always in the morning (9-11AM) to minimize the effect of circadian rhythms

After 1 and 2 weeks from either BMSCs injection or laser irradiation, the rats were anesthetized, sacrificed and parotid glands were dissected out, fixed in 10% neutral buffered formalin solution for 72 hours and then microtechnically processed. Sagittal tissue sections were treated with the following techniques: antigen (PCNA).

2.3. Histological investigations: the tissue sections were stained with hematoxylin and eosin (H & E) (Mayer's hematoxylin)⁽¹⁷⁾. for surveying the histological structure of normal and experimental structure of parotid gland in the different experimental groups of animals.

2.4. Immunohistochemical investigations for the proliferating cell nuclear antigen (PCNA): four to five microns thick sections were cut on tissue adhesive coated slides and tissue sections were stained by commercially available PCNA primary antibody. According to *Akyol et al (1999)*⁽¹⁸⁾, the staining method proceeded as follows: tissue sections were deparaffinized in two changes of xylene for 10 minutes each, rehydrated through graded ethanol, then washed in distilled water for 2 minutes, followed by washing in phosphate buffer saline (PBS) for 5 minutes. To block the endogenous peroxidase activity, slides were incubated in a solution of 3% hydrogen peroxide in methanol for 20 minutes, and then washed in PBS for 5 minutes. For antigen retrieval, the slides were heated in a microwave oven at 100°C for three successive trades, 5 minutes each, and then placed in PBS for 5 minutes. Slides were incubated with the primary antibody over night at 4°C. The standard Streptavidin biotinylated peroxidase complex method was performed. The antigen was localized by the addition of diaminobenzidine (DAB) substrate chromogen solution for 5-10 minutes, followed by Mayer's hematoxylin counterstaining. Finally, the slides were dehydrated, cleared and finally mounted with purified Canada balsam (DPX-Sigma).

3. Preparation of bone marrow-derived MSC (Ficoll-Paque technique)⁽¹⁹⁾: bone marrow was harvested by flushing the tibiae and femurs of six-week-old male Sprague-Dawley rats with Dulbecco's modified Eagle's medium (DMEM) supplemented with 10% fetal bovine serum. The nucleated cells were isolated with a density gradient (Ficoll-Paque, Pharmacia)TM and resuspended in complete culture medium supplemented with 1% penicillin- streptomycin. The cells were then incubated at 37°C in 5% humidified CO₂ for 12–14 days as the primary culture for the formation of large colonies.

With development of large colonies (80–90% confluence), the cultures were washed twice with phosphate-buffered saline (PBS) and the stuck cells to the base of the bottle were trypsinized with 0.25% trypsin in 1 mM EDTA for 5 min at 37°C. After centrifugation, the cells were resuspended with serum-supplemented medium and incubated in 50-cm² culture flask (Falcon). The resulting cultures were referred to as the first-passage cultures⁽¹⁹⁾ and the MSCs in culture were characterized by both their adhesiveness and fusiform shape⁽²⁰⁾.

3.1. Laser Irradiation Technique: infrared -diode low level laser, 980 nm wavelength laser (Denlase Device, made in China, Secure Tec Company) apparatus was used. The unit has a contact probe with a laser beam diameter of 1 cm. The extra oral laser probe was perpendicular to the rat parotid gland

lateral side of the head to cover the area of parotid gland. A diode laser with 660 nm wavelength, input power of 100mW was applied to the skin over the parotid area gland, that is the area approximately 1 cm² was irradiated⁽²¹⁾.

3.2. Image Analysis: the immunohistochemically reacted tissue sections were digitized using a

Zeiss Mirax automated slide scanner with an objective of $\times 20$ magnification. *The proliferating cell nuclear antigen (PCNA)* was evaluated using a score corresponding to the sum of the percent of both the frequency of positively reactive cells and the intensity of reaction. The digital image analysis was performed by importing the Mirax files into the image analyser software Visiopharm Integrater System (VIS).

3.3. **Statistical analysis:** the data were tabulated, coded then analyzed using the computer program. The SPSS (Statistical package for social science) version 17.0 was used to compare the immune expression of PCNA in salivary gland tissues with the clinical parameters. The measured values were expressed as mean values \pm SD (standard deviation). The statistical importance of the difference in these values between the different groups was estimated using ANOVA followed by post-hoc tukey. The *p* value less than 0.05 was considered as significant.

III. Results

3.1. Histological features of parotid salivary glands in control versus experimental groups of rats.

3.1.1. Control group (G I): the histological features of parotid glands collected after 1,2 weeks were composed of normal regular parenchyma and connective tissue stroma. The interstitial connective tissue septae, separated the parenchymal tissue into lobes and lobules. The lobes and lobules were mainly composed of tightly packed serous acini, dispersed with some intercalated, striated and secretory ducts. The acinar cells appeared pyramidal in shape with a basally located oval or round basophilic nuclei in deeply eosinophilic cytoplasm. (*Fig. 1*).

3.1.2. Diabetic group (G II):

A. Seven days post diabetes (G II-A): the general parenchymal architecture of the normal gland was massively destructed at the outmost change, where the vast majority of acini showed severe and massive degeneration with their replacement with collagenous tissue while some areas revealed hyaline degeneration (*Figs.2*). The sparsely remaining acini were widely distributed and appeared atrophied while some of the acini revealed degeneration of the central part and so acquired duct-like appearance. The collagen fibers appeared fused together to form glassy dense hyalinized eosinophilic material and such hyalinization was very common in the fibrous tissue which has been laid down as a reactive replacement for the lost parenchymal tissue. The ducts appeared degenerated with discontinuity of their cellular lining, whereas some ductal cells showed paranuclear vacuolations. The ductal elements were of significant higher proportion relative to the remaining secretory end pieces .

B. Fourteen days post-diabetes (G II-B): the parotid gland appeared degenerative but was less severe than that recorded after seven days post-diabetes. The general acinar architecture was mainly preserved, although some diabetic degenerative changes in some acini were also obvious. In general, the proportion of the acini to ducts were closer to normal in contrast to the seven days changes after diabetic induction. The most outstanding injurious changes were the paranuclear vacuolations (*Figs.3*).

3.1.3. Diabetes with stem cells (G III):

A. Seven days post-diabetes (G III-A): the parotid acini appeared with similar size relative to these in the control group but with occasional mild acinar atrophy and relative absence of the acinar paranuclear vacuolations. The acinar cell nuclei were pleomorphic, but some nuclei appeared with open faced. The ductal elements revealed intact architecture, while some striated duct cells showed paranuclear vacuolations. Many dilated blood vessels and capillaries appeared in the periductal area whereas some were scattered between

the acini (*Fig.4*).

B. Fourteen days post-diabetes (G III-B): the gland architecture was relatively intact while the parenchymal elements showed more or less changes than those of seven days of the same group as the acinar cell hyperplasia. The acini were mildly atrophic with some acinar cell vacuolations. The duct appeared relatively intact but with some paranuclear vacuolations in some of the duct cells. (*Fig.5*).

3.3.4. Diabetes with LLLT (G IV).

A. Seven days post-diabetes (G IV-A) the acini were hypertrophic with scanty or even absence of the interacinar spaces. The vast majority of acini acquired ovoid or tubular configuration, while the acinar cell nuclei appeared pyknotic and located close to the basal cell membrane. The ducts revealed prominent shrinkage that was represented by the development of periductal spaces separating the ducts from their surrounding acini. The ductal lumen were collapsed with perinuclear vacuolations in few duct cells (*Figs.6*).

B. Fourteen days post-diabetes (G IV-B): The gland revealed few and scattered interacinar spaces denoting mild to moderate acinar atrophy. While some acini were devoid of vacuoles, other acini showed some perinuclear vacuolations. The acinar cell nuclei appeared pleomorphic with mixture of hyperchromatic and pale staining ones. The ducts appeared with relatively intact architecture, but scanty ones had cellular vacuolations. (*Fig.7*).

3.2.- Immunohistochemical features of parotid salivary glands in control versus experimental groups of the rats: the parotid gland demonstrated mild to moderate immunoreaction to PCNA in laser group (*Fig.8,9*) compared with the stem cell group which demonstrate intense immunoreaction to PCNA in both acini and ducts (*Fig. 10,11*), (table 1) and (diagram 1).

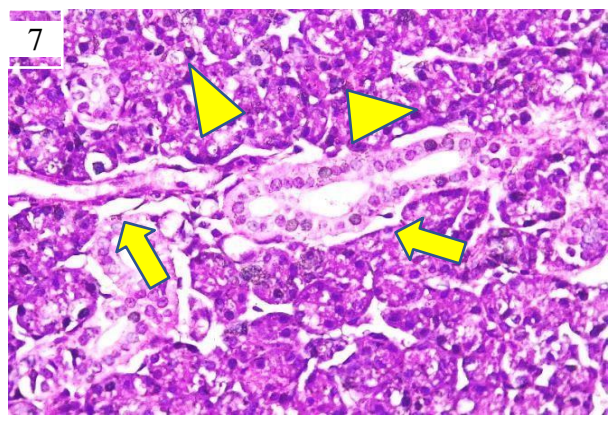
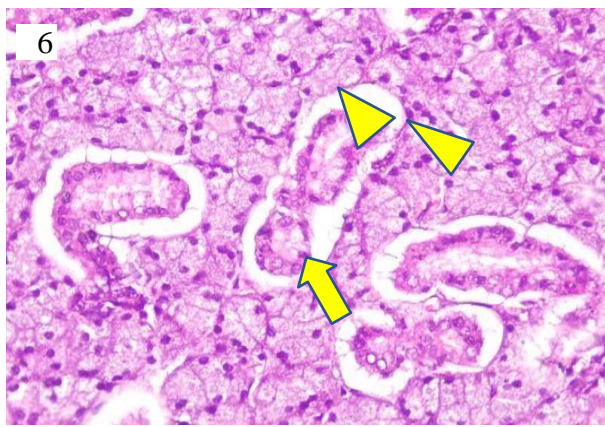
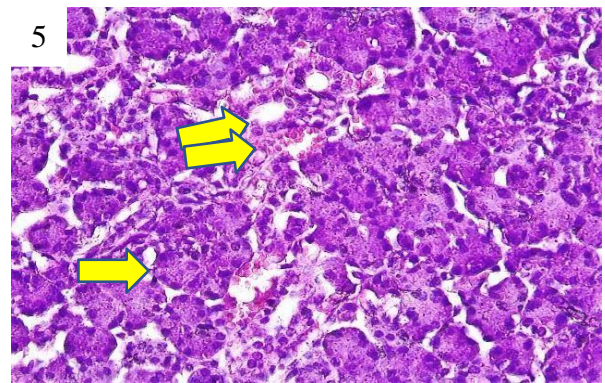
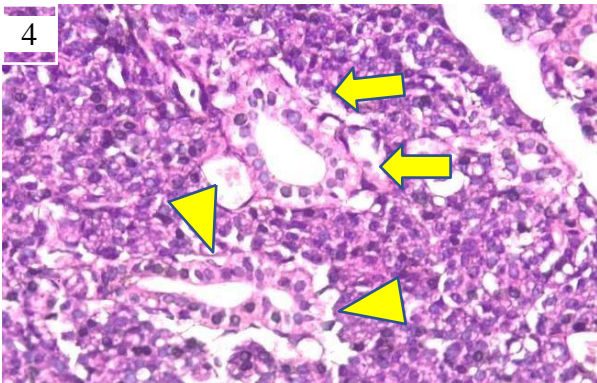
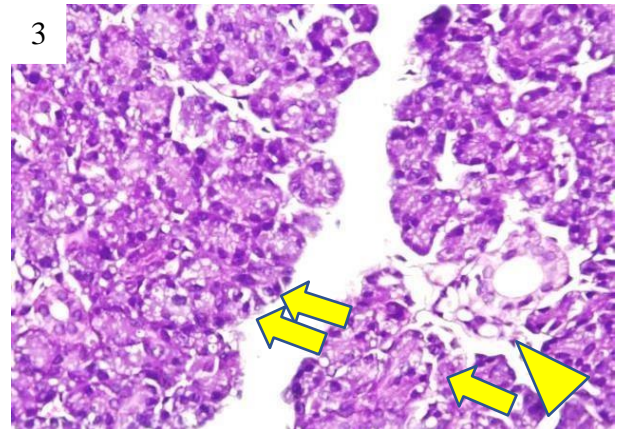
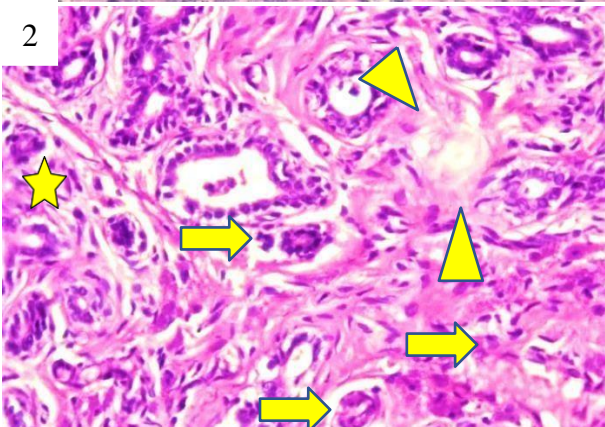
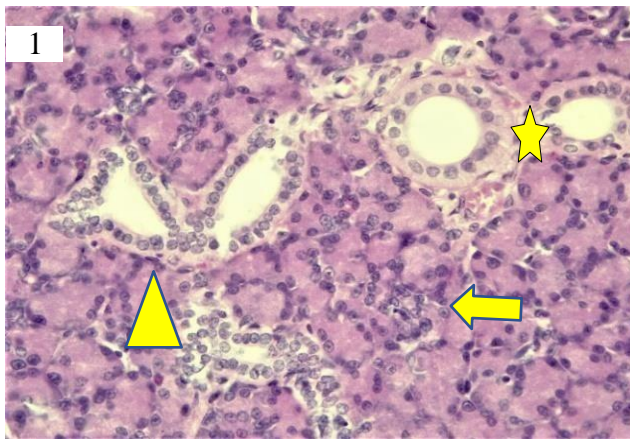


Fig (1): parotid gland of control group (G1) showing normal serous acini (arrow), intercalated (arrow head) and striated ducts surrounded by stroma (star) (H&E stain orig mag. x400).

Fig (2): parotid gland at seven days after diabetes induction (G II-A) showing extensive degeneration of the acinar tissue and its replacement with condensed collagen bundles with occasional focal area of hyaline degeneration (arrowhead), while the remaining acini appear severely atrophied (arrows) and some other acini acquired duct like appearance (stars). (H & E stain, orig Mag. X 400).

Fig (3): parotid gland at fourteen days after diabetes induction (G II-B) showing mild acinar atrophy with many paranuclear vacuolations, while the acinar nuclei appear hyperchromatic and pleomorphic. Some areas show circumductal loss of acinar architecture (arrow), most other acini appear condensed (double arrow). The ducts appear atrophied with some periductal acini appear severely degenerated by vacuolations. (H & E stain, orig Mag. X 400).

Fig (4): parotid gland at seven days after diabetes induction and SC injection (G III-A) showing nearly poorly preserved acinar architecture with frequent paranuclear vacuolations (arrow). The acini show cellular hyperplasia, while their nuclei appear pleomorphic with some are hyperchromatic (arrow head). ducts are surrounded by rich dilated vessels. (H & E stain, orig Mag. X 400).

Fig (5): parotid gland at fourteen days after diabetes induction and SC injection (G III-B) showing of normal acinar architecture (arrow) with occasional mild acinar atrophy and periductal dilated blood vessels (double arrows) (H & E stain, orig Mag. X 400)

Fig (6): parotid gland at seven days after diabetes induction and LLLT exposure (G IV-A) showing considerable acinar hypertrophy. The duct cells appear shrunken, with unstained periductal clear area (arrow head) with almost occluded lumen and some duct cell showing apical vacuolations (arrows). (H & E stain, orig Mag. X 400)

Fig (7): parotid gland at fourteen days after diabetes induction and LLLT exposure (G IV-B) showing loss of regular acinar architecture mild acinar atrophy with some acinar cell vacuolations (arrow). The acinar cell nuclei appear pleomorphic with variable degree of nuclear hyperchromatism (arrow head). (H & E stain, orig Mag. X 400)

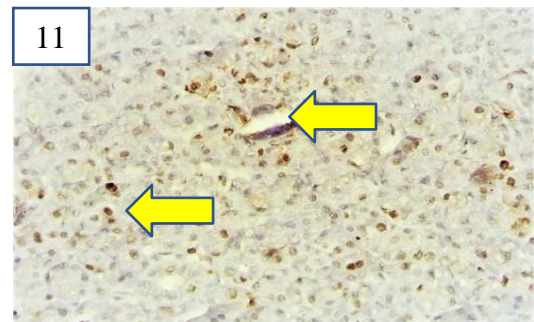
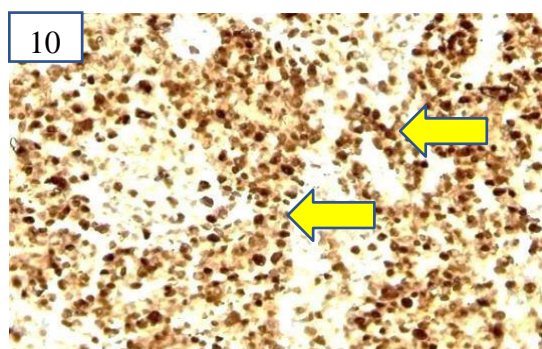
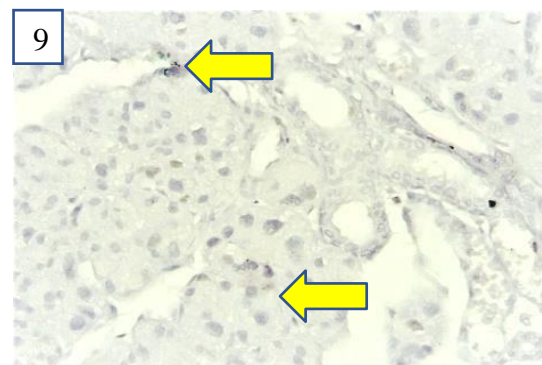
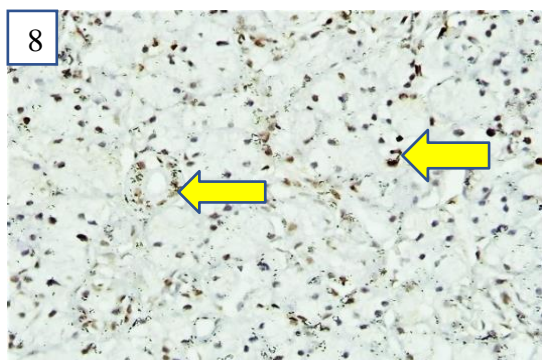


Fig (8): parotid gland at seven days after diabetes induction and SC injection (G III-A) showing moderate immunoreaction (arrow). (PCNA, orig Mag. X 400).

Fig (9): parotid gland at seven days after diabetes induction LLLT (G IV-A) showing slight immunoreaction (arrow) . (PCNA, orig Mag. X 400). Fig (10): parotid gland at fourteen days after diabetes induction and SC injection (G III-B) showing sever intense immunoreaction *in acini and duct* (arrow). (PCNA, orig Mag. X 400).

Fig (11): parotid gland at fourteen days after diabetes induction and LLLT (G IV-B) showing intence immunoreaction in many scattered acini throughout the gland and mild immunoreaction in the ducts(arrow). (PCNA, orig Mag. X 400)

Statistical investigations

1. Statistical analysis for the immunohistochemical reaction of parotid salivary glands in control and experimental groups of rats.

Table (1): Comparison of the percent area of PCNA expression in parotid glands between different groups within 7 & 14 days.

| | Normal group | Diabetic group | Stem cells group | Laser group | P |
|------------------|--------------|----------------|--------------------------|--|---------|
| 7 days Post-hoc | 0±0 | 0±0 | 0.80±0.11 | 0.20±0.03 | <0.001* |
| | | P1=1.00 | P1=<0.001* P2=<0.001* | P1=<0.001* P2=<0.001* P3=<0.001* | |
| 14 days Post-hoc | 0±0 | 1.60±0.23 | 27.50±3.93 | 5.00±0.71 | <0.001* |
| | | P1=0.39 | P1=<0.001* P2=<0.001* | P1=<0.001* P2=0.005* P3=<0.001* | |

Data expressed as mean±SDSD: standard deviation

P: Probability *: significance ≤0.05

Test used: One way ANOVA followed by post-hoc tukey P1: significance vs Normal group

P2: significance vs Diabetic group P3: significance vs Stem cells group P4: significance vs Laser group

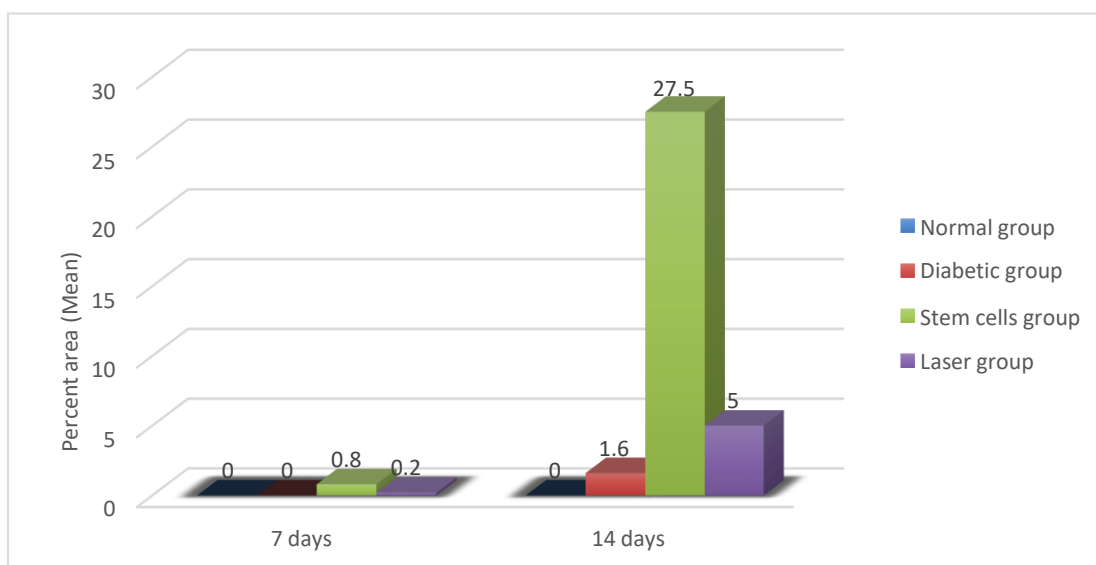


Diagram (1): A histogram representing the mean of percent area of PCNA expression in parotid glands in the

different groups after 7 and 14 days.

IV. Discussion

The parotid glands demonstrated significant diabetic changes after STZ administration that were represented by the degenerative manifestation in both acini and ducts. However, the severity of these diabetic change was variable in the different intervals of the present study. Present study has observed that while the parotid gland appeared degenerated fourteen-days post diabetes, however, such degeneration was less severe than that recorded following seven-days post diabetes. In general, the acinar architecture was mainly preserved, following fourteen-days post diabetes, though some diabetic degenerative changes in some acini were obvious, such as the paranuclear vacuolations. However, the proportion of acini to ducts were closer to normal in contrast to seven days post-diabetes induction. These reactive features may probably indicate that some sort of feedback mechanism may occur thereby resulting naturally in reducing the effect of STZ on salivary gland.

The acinar cell changes of parotid salivary glands showed large numbers of paranuclear vacuoles with shrunken nuclei, loss of acinar structure, severe acinar degeneration with their replacement by collagenous fibrous tissue, while some areas revealed hyaline degeneration; changes that come in accordance with Anderson et al (22).

The basis of diabetogenic degenerative action of STZ is presumed to be mainly based on DNA destruction, and this ultimate fate is reached through one of the three different mechanisms. The first and the most effective mechanism is DNA alkylation, secondly the release of nitric oxide and finally, the generation of the reactive oxygen species (ROS). The DNA alkylation is regarded as the most effective mechanism in the chemical model of laboratory DM⁽²³⁾. The DNA alkylation activity of STZ induced toxic effects in β cells of pancreas lead to their death via the transfer of methyl group from STZ to the β cell DNA molecule. this consequently initiates a chain of events that result in the DNA fragmentation and destruction⁽²⁴⁾.

Reactive oxygen species (ROS) have also been involved in the pathogenesis of diabetes mellitus. Hyperglycemia induced by insulin secretion defect is associated with long term damage, dysfunction, and the failure of various organs⁽²⁵⁾. Hyperglycemia induces the overproduction of superoxide, that is the link between high glucose and pathways responsible for the hyperglycemic damage in diabetic patients^(26,27). Diabetes is typically accompanied by increase in production of the free radicals and/or altered antioxidant defense capabilities, indicating central contribution for ROS in the onset, progression and pathological sequences of diabetes. the ROS has been associated with protein glycation then to protein function impairment. In DM, considerable evidence exists that oxidativdamage is increased⁽²⁸⁾.

Parotid gland was found to be mainly influenced by hyperglycemia at the initial periods of diabetes, have been related to increase in antioxidant enzymatic defense related to ROS⁽²⁹⁾. Increased activity of antioxidant enzymes has been found in several organs including salivary glands of diabetic animals⁽²¹⁾. Persistent hyperglycemia in diabetes may induce considerable production of the free radicals in many tissues⁽³⁰⁾. Free radicals are generated from direct auto-oxidation of glucose and during protein glycosylation⁽³¹⁾. Correlation exists between the status of metabolism control, diabetes mellitus duration and the severity of induced oxidative stress⁽³²⁾.

The cytoplasmic vacuoles detected in the present study in either the acinar or duct cells of parotid glands are comparable to those demonstrated in salivary glands following diabetic induction in the rats⁽³³⁾. The cytoplasmic cell vacuolation has been reported to occur in the rat parotid gland whether it is resting or secreting, and it was indicated that the prolonged strong parasympathetic stimulation, especially after acinar degranulation, has increased the tendency for acinar cell vacuolations⁽³³⁾. On the other hand, this cytoplasmic vacuolations have been presumed to reflect physiopathological state in the affairs from the artificial process of stimulating the nerve electrically⁽³⁴⁾. Alternatively, the parotid acinar cell cytoplasmic vacuolation has been presumed to occur due to imbalance in the cell calcium, and the condition may be reversible in the early stages⁽³⁵⁾.

It was reported that the increased cell function is evidenced by the cell components proliferation or reorganization in a manner suggesting hyperfunction state in response to certain poisons. For instance, the

smooth endoplasmic reticulum proliferates and form complex whorls or gyrations. Both are regarded as adaptive mechanism and interpreted as the cells attempt to increase their ability to detoxify the substance to which they are subjected and evidently cell metabolism becomes increased. This is simulated microscopically by the development of increased macropinocytotic activity resulting in the appearance of numerous cytoplasmic vacuoles ⁽³⁶⁾.

The previous investigations have recorded extensive infiltration with lipid droplets of various magnitudes in H & E sections of parotid gland of diabetic rats versus nondiabetic glands that displayed little or no lipid droplets distribution ⁽³⁷⁾. The clear granule-like lipid droplets in parotid gland sections from diabetic rats suggests that parotid gland cells become dysfunctional during insulin-dependent DM ⁽³⁸⁾. The STZ induced diabetic animals cannot use glucose as energy source during the fasting periods; thus, fat catabolism is activated as alternative energy source ⁽³⁹⁾.

The early onset period after diabetic induction showed severe diabetic degenerative features of acini that had ultimately led to the disappearance of large area of parenchymal elements of the gland. The absent acini and ducts were replaced by dense fibrous tissue, while the remaining scattered acini were vacuolated and showed signs of degeneration these changes were also reported by Denewar & Amin, 2020 ⁽³³⁾. The mechanism underlying collagen abnormalities in diabetic parotid gland is poorly understood. A relationship does exist between STZ-induced diabetes and both ROS and type I collagen organization in parotid gland. Glucose was found to play important role in the accumulation of collagen in the tissues ⁽⁴⁰⁾. Hyperglycemic state leads to advanced glycation and product formation in matrix components and accelerates the crosslinking between collagen fibers. The increased collagen deposition contributes to increased stiffness of tissues in diabetic subjects because of the changes in both the structure and organization of extracellular matrix ⁽²⁹⁾.

The correlation between antioxidant status and type I collagen deposition in diabetic rats with or without acarbose treatment was performed in previous investigation ⁽³⁷⁾. Acini in parotid gland of diabetic state were more widely spaced and showed higher level of collagen deposition and collagen fibers were stained in parotid tissue compared with nondiabetic state. Type I collagen existed between and around ducts, acini nerves and into the walls of arteries and veins ⁽³⁷⁾. These findings were in a line with the findings of the present study.

Sections stained by H&E of diabetic rat parotid glands were extensively infiltrated by lipid droplets of various magnitudes in contradistinction to little or even no distribution of lipid droplets in the nondiabetic parotid gland ⁽³⁷⁾. Streptozotocin-induced diabetic animals cannot use glucose as energy source during fasting period, thus fat catabolism is activated as alternative source ⁽⁴¹⁾.

Clear granule-like structures have been identified in parotid gland sections from diabetic rats by Anderson ⁽⁴²⁾. These findings suggest that parotid gland cells become dysfunctional during insulin-dependent diabetes mellitus. Reduction in size and frequency of lipid droplets with partial reversal of the observed biochemical changes were observed by application of acarbose treatment, a drug able to reduce some of the damage induced by diabetes mellitus ⁽³⁷⁾.

The development of unstained vacuoles attached to the nuclear membrane, simulating negative Golgi image surrounded by deeply eosinophilic cytoplasm were noted by testosterone administration in posterior lingual salivary glands ⁽⁴³⁾. Extensive cytoplasmic vacuolization were noted following oestrogen or progesterone administration in granular convoluted tubules in rat submandibular and parotid glands. The parotid gland acini with diabetic group were higher level of collagen deposition type I collagen occurred around ducts, acini, nerves and in arterial and venous walls and thick densely stained collagen bundles occurred around ducts, whereas thin and delicate fibres were seen around acini and nerves. Diabetes mellitus is metabolic disease affects many organs and in salivary glands an alteration in glycolytic enzyme activity ^(44,45) and in antioxidant parameters ⁽⁴⁶⁾. These changes have been reported in association with diabetes and have also been related to increased collagen deposition described in the heart of diabetic rats ⁽⁴⁰⁾.

Type I collagen content was increased in parotid gland of diabetic rats ⁽³⁷⁾, this is in agreement with the

findings for heart and kidney in streptozotocin diabetic rat⁽⁴⁷⁾ The acarbose treatment in diabetic rats reduced the amount of collagen into similar level as the non-diabetic group⁽³⁷⁾.

-Positive correlation between the amount of type 1 collagen and the oxidative parameters which was also suggested by Baynes⁽⁴⁸⁾. Acini in parotid gland of diabetic rats were widely spaced and exhibited higher levels of collagen deposition. Type 1 collagen was found in diabetic animals around ducts, acini with staining pattern and are thick and densely stained collagen bundles around ducts but were thin and delicate fibres around acini and nerves⁽³⁷⁾.

Stain pattern in diabetic gland revealed thick and densely packed collagen bundles around ducts, but thin and delicate around acini which was also noted in previous investigation⁽³⁷⁾. Alterations in glycolytic enzyme activity and antioxidant parameters have been reported to be associated with diabetes^(29, 32). These changes have also been related to increased collagen deposition in heart of diabetic rats⁽⁴⁰⁾. A previous study has reported a positive relation between type I collagen and oxidative stress parameters⁽⁴⁹⁾, whereas other has reported increased level of glycoxidation products in collagen which can be attributed to increases in glycation and oxidative stress⁽⁵⁰⁾.

In the present study the local administration of bone marrow-derived mesenchymal stem cells (BMDSCs) to parotid gland in diabetic animals has relatively relieved the diabetic manifestations. Concerning one-week interval subgroup, the relief of diabetic features was significant when compared to the same period in the diabetic group G II that was represented by better organization of acinar architecture and less acinar and ductal perinuclear vacuolations. However, some diabetic features including vacuolations and atrophy as well as irregular acinar architecture were still apparent⁽⁵⁰⁾.

The SCs group demonstrated significant expression of PCNA in many acinar and ductal cells, indicating prominent mitotic activity in the vast majority of both acinar and ductal cells. This prominent cellular proliferation was also mentioned in the previous investigation that recorded significant increase in the proliferating cells of BMDSCs-treated mice in parotid gland with degenerative manifestations, induced via radiation exposure⁽⁵¹⁾.

In the current study, the degenerative changes in the parotid glands of diabetic rats were reduced after the glands were subjected to low-level laser therapy. The glands have relatively regained the histological features as that of control rats. This architectural enhancement associated with LLLT was also observed in the diabetic group subjected to low-level laser irradiation which reestablished serous acini normal appearance except for small intracytoplasmic vacuoles that were observed in few acini. These observations in the present study were also in agreement with that noted in previous investigation⁽⁵²⁾.

Another study has showed that low-power laser therapy can decrease the blood glucose levels of diabetic animals, as well as modulate the enzymatic antioxidant system of salivary glands of streptozotocin-induced diabetic rats. Additionally, they stated that the decrease in blood glucose levels in diabetic animals after laser therapy could be linked to the action of insulin growth factor 1 (IGF-I). Moreover, they declared that the low-level laser therapy has increased the total protein content of parotid gland of rats, reduced changes in the catalase activity in parotid and submandibular glands of diabetic rats and promoted the cell proliferation and expression of antiapoptotic proteins in cells of rat parotid gland⁽⁵³⁾. It has been thought that the laser improves the local microcirculation, induces the glandular cell proliferation, and increases the cell respiration, ATP production, protein syntheses, and intracellular calcium level⁽⁵⁴⁾.

In the present study, the local intraparotid BMSCs injection has led to PCNA proliferation index upregulation as compared to the low-level laser therapy and diabetic group. This observation was in accordance with the results recorded in previous study, which noted increased proliferative index as marked by increased PCNA expression and decreased apoptotic index as marked by TUNEL in the irradiated submandibular gland tissues treated with intraglandular BMSCs⁽⁵⁵⁾.

V. Conclusion

The BMSCs can reach the parotid glands and laser stimulation can enhance the healing potential and the proliferative capacity of the parotid gland cells in diabetic cases.

The BMSCs and the LLLT (laser bio stimulation) can be used as an adjunctive treatment modality for alleviating the degenerative changes of salivary glands associated with diabetes mellitus and to overcome the salivary glands complications associated with diabetic patients, thus enhancing their quality of life.

References

- [1] **Kerner W, Brückel J, German Diabetes Association.** Definition, Classification And Diagnosis Of Diabetes Mellitus. *Exp Clin Endocrinol Diabetes*, 2014; 122 (7): 384- 6.
- [2] **Guthrie RA, Guthrie DW.** Pathophysiology of Diabetes Mellitus. *Crit Care Nurs Q*, 2004; 27(2): 113-45.
- [3] **Anderson LC, Johnson DA.** Effects of alloxan diabetes on rat parotid gland and saliva. *Comp Biochem physiol*, 1981; 70: 725-30.
- [4] **Hand AR, Weiss RE.** Effects of streptozotocin diabetes on the rat parotid gland. *Lap Invest*, 1984; 51(4): 429-40.
- [5] **Szkudelski T.** The Mechanism of Alloxan and Streptozotocin Action in B Cells of the Rat Pancreas. *Physiol Res*, 2001; 50(6): 537-46.
- [6] **Ogawa M, Tsuji T.** Functional Salivary Gland Regeneration As The Next Generation Of Organ Replacement Regenerative Therapy. *Odontology*, 2015; 103(3): 248–57.
- [7] **Coppes RP, Stokman MA.** Stem Cells And The Repair Of Radiation-Induced Salivary Gland Damage. *Oral Dis*, 2011; 17(2): 143–53.
- [8] **Granero-Moltó F, Weis JA, Miga MI, Landis B, Myers TJ, O’Rear L, et al.** Regenerative Effects Of Transplanted Mesenchymal Stem Cells In Fracture Healing. *Stem Cells*, 2009; 8(27): 1887–98.
- [9] **Lin CY, Chang FH, Chen CY, Huang CY, Hu FC, Huang WK, et al.** Cell Therapy For Salivary Gland Regeneration. *J Dent Res*; 2011; 90(3): 341–6.
- [10] **di Nicola M, Carlo-Stella C, Magni M, Milanese M, Longoni PD, Matteucci P, et al.** Human Bone Marrow Stromal Cells Suppress T-Lymphocyte Proliferation Induced By Cellular Or Nonspecific Mitogenic Stimuli. *Blood*, 2002; 99(10): 3838–43.
- [11] **Juras DV, Luka J, Cekić-Arambain A, Vidović A, Canjuga I, Sikora M, et al.** Effects Of Low-Level Laser Treatment On Mouth Dryness. *Coll Antropol*, 2010; 34 (3): 1039–43.
- [12] **Lončar B, Mravak Stipetić M, Baričević M, Risović D.** The Effect Of Low-Level Laser Therapy On Salivary Glands In Patients With Xerostomia. *Photomed Laser Surg*, 2011; 29(3): 171–5.
- [13] **Furman BL.** Streptozotocin-Induced Diabetic Models in Mice and Rats. *Curr Protoc Pharmacol*, 2015; 70(1): 5.47.1-5.47.20.
- [14] **Wang F, Chen TS, Xing D, Wang JJ, Wu YX.** Measuring Dynamics Of Caspase-3 Activity In Living Cells Using FRET Technique During Apoptosis Induced By High Fluence Low-Power Laser Irradiation. *Lasers Surg Med*, 2005; 36(1): 2–7.
- [15] **Hwang D, Seo S, Kim Y, Kim C, Shim S, Jee S, et al.** Selenium Acts As An Insulin-Like Molecule

- For The Down-Regulation Of Diabetic Symptoms Via Endoplasmic Reticulum Stress And Insulin Signalling Proteins In Diabetes-Induced Non-Obese Diabetic Mice. *J Biosci*, 2007; 32 (4): 723–35.
- [16] **Huang S, Xu L, Zhang Y, Sun Y, Li G.** Systemic and Local Administration of Allogeneic Bone Marrow-Derived Mesenchymal Stem Cells Promotes Fracture Healing in Rats. *Cell Transplant*. 2015;24(12):2643-55.
- [17] **Bancroft JD, Gamble M.** Theory and Practice of Histological Technique. Churchill Livingstone. Edinburgh London New York Oxford Philadelphia St Louis Sydney Toronto. 2002, 5th Ed.:125-242.
- [18] **Akyol G, Dursun A, Poyraz A, Uluoglu O.** P53 And Proliferating Cell Nuclear Antigen (PCNA) Expression In Non Tumoral Liver Diseases. *Pathol Int*, 1999; 49(3): 214-21.
- [19] **Alhadlaq A, Mao JJ.** Mesenchymal Stem Cells: Isolation and Therapeutics. *Stem Cells Dev*, 2004; 13(4): 436–48.
- [20] **Rocheffort GY, Vaudin P, Bonnet N, Pages J-C, Domenech J, Charbord P, et al.** Influence Of Hypoxia On The Domiciliation Of Mesenchymal Stem Cells After Infusion Into Rats: Possibilities Of Targeting Pulmonary Artery Remodeling Via Cells Therapies? *Respi Res*, 2005; 6(1):125.
- [21] **Simões A, Ganzerla E, Yamaguti PM, de Paula Eduardo C, Nicolau J.** Effect Of Diode Laser On Enzymatic Activity Of Parotid Glands Of Diabetic Rats. *Lasers Med Sci*, 2009; 24(4): 591–6.
- [22] **Anderson LC, Garrett JR.** Lipid accumulation in the major salivary glands of streptozotocin-diabetic rats. *Arch Oral Biol*. 1986;31(7):469-75.
- [23] **Radenković M, Stojanović M, Prostran M.** Experimental Diabetes Induced By Alloxan And Streptozotocin: The Current State Of The Art. *J Pharmacol Toxicol Methods*, 2016; 78: 13–31..
- [24] **Lenzen S.** The Mechanisms Of Alloxan- And Streptozotocin-Induced Diabetes. *Diabetologia*, 2008; 51(2): 216–26.
- [25] **Expert Committee on the Diagnosis and Classification of Diabetes Mellitus.** Report Of The Expert Committee On The Diagnosis And Classification Of Diabetes Mellitus. *Diabetes Care*, 2003;26 (1):5-20.
- [26] **Brownlee M.** Biochemistry And Molecular Cell Biology Of Diabetic Complications. *Nature*, 2001; 414(6865): 813-20.
- [27] **Giardino I, Edelstein D, Brownlee M.** BCL-2 Expression Or Antioxidants Prevent Hyperglycemia-Induced Formation Of Intracellular Advanced Glycation Endproducts In Bovine Endothelial Cells. *J Clin Invest*. 1996; 97(6):1422-8.
- [28] **West IC.** Radicals And Oxidative Stress In Diabetes. *Diabet Med*, 2000;17(3):171-80.
- [29] **Ibuki FK, Simões A, Nogueira FN.** Antioxidant Enzymatic Defense In Salivary Glands Of Streptozotocin-Induced Diabetic Rats: A Temporal Study. *Cell Biochem Funct*, 2010; 28(6): 503–8.
- [30] **Kakkar R, Kalra J, Mantha, SV, Prasad K.** Lipid Peroxidation And Activity Of Antioxidant Enzymes In Diabetic Rats. *Mol Cell Biochem*, 1995; 151: 113–119.
- [31] **Bonnefont-Rousselot D, Pastard JP, Jaudon MC, Delattre J.** Consequences Of The Diabetic Status On The Oxidant/Antioxidant Balance. *Diabetes & Metab (Paris)*, 2000; 26: 163-176.
- [32] **Nogueira J, Lecuona A, Rodriguez P.** Limits on the resolution of correlation PIV iterative methods. Fundamentals. *Exp Fluids*, 2005; 39(2): 305-13.
- [33] **Denewar M, Amin E.** Role Of Bone Marrow-Derived Mesenchymal Stem Cells On The Parotid

- Glands Of Streptozotocin Induced Diabetes Rats . *J Oral Biol Craniofac Res.* 2020; 10(2): 33–7.
- [34] **Garrett JR.** The Proper Role Of Nerves In Salivary Secretion: A review. *J Dent Res*, 1987, 66(2): 387-97.
- [35] **Leslie BA, Putney Jr JW.** Ionic: Mechanisms in Secretagogue induced Morphological Changes in Rat Parotid Gland. *J cell Biol*, 1983; 97(4): 1119-30.
- [36] **Trump B, Janijan D.** The pathogenesis of cytologic vacuolization in sucrose nephrosis. An electron microscopic and histochemical study. *Lab Invest*, 1962; 11: 395-411.
- 37- **Deconte S, Oliveira R, Calábria L, Oliveira V, Gouveia N, Moraes S, et al.** Alterations Of Antioxidant Biomarkers And Type I Collagen Deposition In The Parotid Gland Of Streptozotocin-Induced Diabetic Rats. *Arch Oral Biol*, 2011; 56(8): 744-51.
- 38- **Anderson L.** Parotid Gland Function in Streptozotocin-diabetic Rats. *Am J Physiol*, 1987; 245: 431-7.
- 39 - **Fritsche L, Weigert C, Haring HU, Lehman R.** How Insulin Receptor Substrate Proteins Regulate The Metabolic Capacity Of The Liver--Implications For Health And Disease. *Curr Med Chem*, 2008; 15(13): 1316- 29.
- 40 - **Kohda Y, Kanematsu M, Kono T, Terasaki F, Tanaka T.** Protein O-Glycosylation Induces Collagen Expression And Contributes To Diabetic Cardiomyopathy In Rat Cardiac Fibroblasts. *J Pharmacol Sci*, 2009; 111(4): 446-50.
- 41-. **Fritsche L, Weigert C, Haring HU, Lehman R.** How Insulin Receptor Substrate Proteins Regulate The Metabolic Capacity Of The Liver--Implications For Health And Disease. *Curr Med Chem*, 2008; 15(13): 1316- 29
- 42- **Anderson L.** Parotid Gland Function in Streptozotocin-diabetic Rats. *Am J Physiol*, 1987; 245: 431-7.
- 43- **Hani SM.** The Influence Of Testosterone Administration On The Histology And Carbohydrate Histochemistry Of The Rat Salivary Glands. *Al-Azhar Dental J*, 2000; 7(2):159-78.
- 44- **Nicolau J, Souza DN, Nogueira FN.** Activity, Distribution And Regulation Of Phosphofructokinase In Salivary Gland Of Rats With Streptozotocin-Induced Diabetes. *Braz Oral Res*, 2006; 20(2):108-13.
- 45- **Nogueira FN, Santos MF, Nicolau J.** Influence Of Streptozotocin-Induced Diabetes On Hexokinase Activity Of Rat Salivary Glands. *J Physiol Biochem*, 2005; 61(3): 421-7.
- 46- **Reznick AZ, Shehadeh N, Shafir Y, Nagler RM.** Free Radicals Related Effects And Antioxidants In Saliva And Serum Of Adolescents With Type 1 Diabetes Mellitus. *Arch oral biol*, 2006; 51(8): 640—8.
- 47- **Fujisawa G, Okada K, Muto S, Fujita N, Itabashi N, Kusano E, et al.** Spironolactone Prevents Early Renal Injury In Streptozotocin-Induced Diabetic Rats. *Kidney Int*, 2004; 66(4): 1493-502.
- 48- **Baynes JW.** Role Of Oxidative Stress In Development Of Complications In Diabetes. *Diabetes*. 1991; 40(4): 405-12.
- 49- **Baynes JW.** Role Of Oxidative Stress In Development Of Complications In Diabetes. *Diabetes*. 1991;40(4):405-12. 50- **Waleed M, Rasha M, Taha L, Laila S.** Effect Of Bone Marrow-Derived Stem Cells On The Submandibular Salivary Glands Of Streptozotocin-Induced Diabetic Rats. *Suez Canal Univ Med J*, 2017; 20 (1), 29-37.

- 51- **Sumita Y, Liu Y, Khalili S, Maria OM, Xia D, Key S, et al.** Bone Marrow-Derived Cells Rescue Salivary Gland Function In Mice With Head And Neck Irradiation. *Int J Biochem Cell Biol*, 2011; 43(1): 80–7.
- 52- **Hoda A, Sahar M. El-Hadidi D, Eman H, Tarek I.** Laser Biostimulation Of Salivary Glands In Diabetic Rats. *Middle East J Med Genetics*, 2017, 6:41–47.
- 53- **Ibuki FK, Simões A, Nicolau J, Nogueira FN.** Laser Irradiation Affects Enzymatic Antioxidant System Of Streptozotocin-Induced Diabetic Rats. *Lasers Med Sci*, 2013; 28(3): 911–8.
- 54- **Palma LF, Gonnelli FAS, Marcucci M, Dias RS, Giordani AJ, Segreto RA, et al.** Impact Of Low-Level Laser Therapy On Hyposalivation, Salivary Ph, And Quality Of Life In Head And Neck Cancer Patients Post-Radiotherapy. *Lasers Med Sci*, 2017; 32(4): 827–32.
- 55- **Lim JY, Yi T, Choi JS, Jang YH, Lee S, Kim HJ, et al.** Intraglandular Transplantation Of Bone Marrow-Derived Clonal Mesenchymal Stem Cells For Amelioration Of Post-Irradiation Salivary Gland Damage. *Oral Oncol*, 2013; 49(2): 136–43.